Polarization and retinal image quality estimates in the human eye

Juan M. Bueno and Pablo Artal

Laboratorio de Optica, Departamento de Física, Universidad de Murcia, Campus de Espinardo (Edificio C), 30071 Murcia, Spain

Received April 7, 2000; revised manuscript received September 19, 2000; accepted September 26, 2000

We have previously studied how polarization affects the double-pass estimates of the retinal image quality by using an imaging polarimeter [Opt. Lett. **24**, 64 (1999)]. A series of 16 images for independent combinations of polarization states in the polarimeter were recorded to obtain the spatially resolved Mueller matrices of the eye. From these matrices, double-pass images of a point source for light with different combinations of incoming (first-pass) and outcoming (second-pass) polarization states were reconstructed and their corresponding modulation transfer functions were calculated. We found that the retinal image or, alternatively, the ocular aberrations, are nearly independent of the state of polarization of the incident light (in the first pass). This means that a significant improvement in the ocular optics by using a specific type of polarized light could not be achieved. However, quite different estimates of the retinal image quality are obtained for combinations of polarization states in both the first and the second passes in the double-pass apparatus. © 2001 Optical Society of America

OCIS codes: 120.5410, 170.3880, 330.5370.

1. INTRODUCTION

For more than 40 years, the double-pass method has been used successfully to estimate the optical performance of the human eye for different conditions.[1–9] In this technique a point source is imaged on the retina, and the light reflected back from the eye is imaged a second time (see Ref. 10 for a general review). The ocular modulation transfer function (MTF) is calculated from these double-pass images. In general, the effects of polarization due to the different components of the eye and the apparatus itself in those results were thought to be negligible. However, the ocular media and the retina change the polarization state of the incident light in a complicated way.[11] The cornea is highly birefringent.[12–14] This property generally increases along the radius and is associated with the birefringence that is due to each individual fiber (intrinsic birefringence) and the stack formed by the lamellae (form birefringence). Unlike that in the cornea, the total birefringence of the lens may be neglected because there is an effect of cancellation between the negative form birefringence that arises from the arrangement of the fiber cell membranes and the positive intrinsic birefringence that is due to intercellular organization.[15,16] The retinal structure is more complex and has properties of birefringence, dichroism, and depolarization.[17–23] This suggests that every technique based on collecting the light scattered back in the retina will be potentially affected by polarization, and that, in particular, these changes may affect the estimates of the retinal image quality obtained by double-pass techniques. In addition to the effect that is due to the polarization of the eye itself, the experimental apparatus usually incorporates polarization components for various purposes. For instance, it was suggested that better estimates of image quality could be obtained by placing parallel polarizers in both first and second passes,[24] and a configuration of crossed linear polarizers in the first and second passes was proposed to eliminate the corneal reflex. This approach is also in use in some of the Hartmann–Shack wave-front sensors[25,26] to measure ocular aberrations. On the other hand, a different approach has been used for imaging the polarization properties of the retinal nerve fibers, which can be an early indication of glaucoma.[23]

The aim of this paper is to study how double-pass estimates of the retinal image quality are affected by the polarization state of the light. We used a double-pass imaging polarimeter[27] to measure spatially resolved Mueller matrices (MM's) of the living human eye obtained from a series of 16 double-pass images corresponding to different combinations of generator–analyzer polarization states. From these MM's, the effect of the polarization of the incident light was evaluated by simple matrix calculations. The procedure allows us to estimate the retinal image quality by isolating the polarization effects of the eye and the system in both the incoming and the outcoming light.

2. MUELLER-MATRIX IMAGING POLARIMETER

A MM [M_{ij} $(i, j = 0, 1, 2, 3)$] contains all the polarization properties of a system. It transforms any incident light, characterized by a Stokes vector, into an outcoming Stokes vector that describes the light after interacting with the media. Element M_{00} represents the emergent intensity when the incident light is nonpolarized. Elements M_{01}, M_{02}, and M_{03} describe dichroism (attenuation between two orthogonal polarization states). Elements of the first column contain information about the polarizance (the possibility of increasing the degree of polarization of a nonpolarized incident light). The lower-

0740-3232/2001/030489-08$15.00

right 3×3 submatrix indicates the retardation introduced by the birefringent structures of the system.

The apparatus used to obtain spatially resolved MM's of the living eye was previously described in Ref. 27 (Fig. 1 here). This is a polarimeter incorporating a pair of liquid-crystal variable retarders (LCVR's) (Thorlabs, PDA50/M) adapted to an ophthalmoscopic double-pass setup.[3] Briefly, the eye is illuminated by a point source, O, generated by a 633 nm He–Ne laser. The size of the beam entering the eye (either 2 or 5 mm in diameter) is controlled by aperture AP_1, acting as entrance pupil in the first pass. Both the polarization-state generator, PSG, and the polarization-state analyzer, PSA, include a LCVR and a removable quarter-wave plate. The double-pass image, O″, is formed by a photographic objective on the CCD plane of a scientific-grade slow-scan camera (SpectraSource MCD1000). An afocal system, 148-mm lenses L_2 and L_3, and an optional trial lens permit the correction of defocus and astigmatism, respectively. The maximum irradiance on the cornea during exposures was less than 250 nW/cm^2, well below the maximum permissible exposure limit.[28] When the LCVR's and driven with appropriate voltages, only three completely independent states of polarization can be produced. When the two additional quarter-wave plates are placed in the entrance and exit optical pathways, the fourth required independent polarization state is produced.[27]

Measurements were carried out in three normal subjects: AG, JB, and PA: 26, 27, and 37 years old, respectively. Accommodation was paralyzed and the pupil dilated with two drops of tropicamide (1%). The subject's head was stabilized by means of a bite bar mounted on a three-axis micrometric stage. To determine the best refractive state, each subject looked for the best focus by moving lens L_2 while staring at the (conveniently attenuated) point source directly, until he saw the smallest and the brightest point source. This focus was confirmed by recording double-pass images for different focus settings around the best subjective focus.

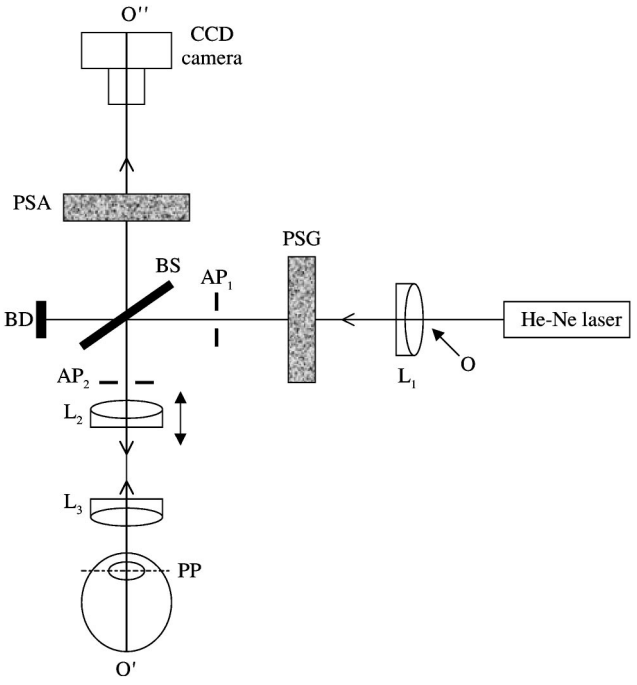

Fig. 1. Simplified diagram of the MM double-pass imaging polarimeter. L_1, L_2, and L_3, achromatic lenses; AP_1 and AP_2, apertures acting as stop for the first and the second pass, respectively; PSG, polarization-state generator; PSA, polarization-state analyzer; BS, beam splitter; PP, pupil plane; O, point source; O′, retinal image; O″, double-pass image.

A series of 16 double-pass retinal images of a point source (4 s exposure time and 256×256 pixels with 16 bits/pixel) were recorded for the PSG–PSA combinations of polarization states. A background image obtained by placing a black diffuser in place of the eye was also recorded. Owing to possible fluctuations in the intensity of the source and the presence of noise in the images, every double-pass image was corrected as indicated in Ref. 29. Figure 2 shows, as an example, double-pass retinal images corresponding to 16 independent combinations of polarization states PSG–PSA, recorded at the fovea with an artificial pupil 2 mm in diameter. Polarization states H, V, 45, and C are associated with horizontal, vertical, 45-deg linear and right-circular light, respectively. Images HH and VV are similar to those recorded with parallel polarizers in the first and second passes. Images HV and VH correspond to the case of images recorded with crossed polarizers.

From each set of 16 images, the spatially resolved MM was obtained by a matrix inversion method.[27] Figure 3 shows an example of the spatially resolved MM obtained with 2-mm pupil diameter. Each image corresponds to one element of the matrix and subtends 59 arc min. The matrix elements are normalized to the maximum of element M_{00}. This matrix contains information about the double pass through ocular media and the retinal reflection and is a powerful tool for predicting the polarization-related ocular aberrations. Spatially resolved MM's are the generalization of the scalar point-spread function in the Mueller formalism.[30,31]

3. RECONSTRUCTION OF DOUBLE-PASS IMAGES FROM SPATIALLY RESOLVED MUELLER MATRICES

From the MM, double-pass images of a point source for different combinations of incoming and outcoming polarization states are obtained by

$$\begin{pmatrix} S_0^{(mn)} \\ S_i^{(mn)} \\ S_2^{(mn)} \\ S_3^{(mn)} \end{pmatrix} = M_{\mathrm{PSA}}^{(n)} \begin{bmatrix} M_{00} & M_{01} & M_{02} & M_{03} \\ M_{10} & M_{11} & M_{12} & M_{13} \\ M_{20} & M_{21} & M_{22} & M_{23} \\ M_{30} & M_{31} & M_{32} & M_{33} \end{bmatrix} \times S(m) = M_{\mathrm{PSA}}^{(n)} M M_{\mathrm{eye}} S(m) \qquad (1)$$

where M_{ij} $(i, j = 0, 1, 2, 3)$ are the elements of the spatially resolved MM of the eye (MM_{eye}), $S(m)$ is the incoming polarization state, $M_{\mathrm{PSA}}^{(n)}$ is the MM of the PSA, and $s_0^{(mn)}$ is the intensity of the emerging Stokes vector, which corresponds to the double-pass image. A schematic illustration of the represented experiment is depicted in Fig. 4(a). For example, if the eye is placed between parallel and crossed linear polarizers, double-pass images are reconstructed by

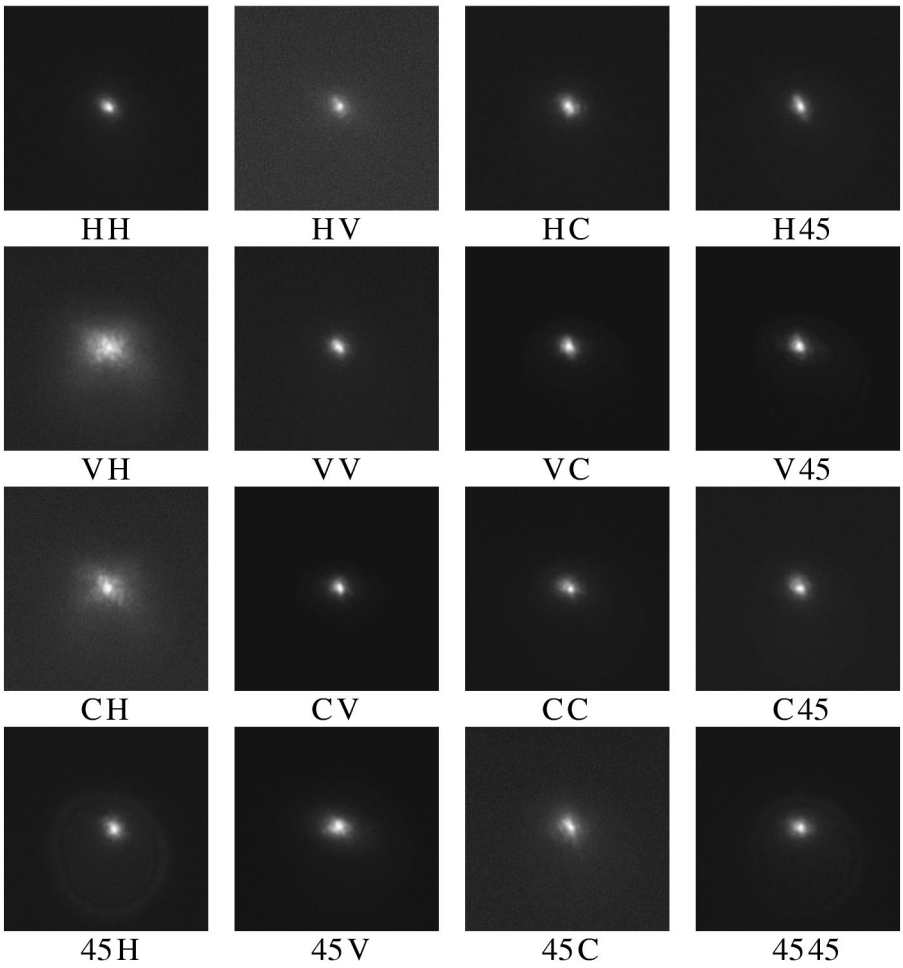

Fig. 2. Series of 16 double-pass retinal images recorded with the polarimeter, corresponding to independent PSG–PSA combinations for subject JB and 2-mm pupil diameter. Each image subtends 59 arc min.

$$I^{D-P}_{\text{parallel}} = M_{00} + M_{01} + M_{10} + M_{11}$$
$$I^{D-P}_{\text{crossed}} = M_{00} + M_{01} - M_{10} - M_{11}. \tag{2}$$

It is also of interest to reconstruct double-pass images when only the polarization state of the first pass (incoming beam) is modified [Fig. 4(b) shows a schematic diagram of this situation]. The double-pass image resulting from the interaction between the incident polarized light and the eye will be the first element of the Stokes vector, given by

$$\begin{pmatrix} S_0^{(m)} \\ S_1^{(m)} \\ S_2^{(m)} \\ S_3^{(m)} \end{pmatrix} = MM_{\text{eye}} S(m). \tag{3}$$

Since every possible polarized incident light over the Poincaré sphere (with azimuth χ and ellipticity ϕ) can be described by a Stokes vector $S(m) = S_{\text{IN}}$,

$$S_{\text{IN}} = \begin{pmatrix} 1 \\ \cos 2\chi \cos 2\phi \\ \sin 2\chi \cos 2\phi \\ \sin 2\phi \end{pmatrix}, \tag{4}$$

the double-pass images for any given incident light are obtained as

$$I^{(m)}_{(\chi,\,\phi)} = S_0^{(m)} = M_{00} + \cos 2\chi \cos 2\phi M_{01} + \sin 2\chi \cos 2\phi M_{02} + \sin 2\phi M_{03}. \tag{5}$$

With this procedure, retinal images for any arbitrary polarization state are obtained from the spatially resolved MM. Subsequently, the MTF and the Strehl ratio were obtained for each image reconstructed (see Ref. 32 for details on how the MTF and the Strehl ratio were computed from double-pass images).

4. RESULTS

A. Double-Pass Images Reconstructed for Different Combinations of Polarization States in Both Passes

Figure 5 shows double-pass images reconstructed from the MM for different combinations of polarization states in the first and second passes (subject JB with a 2-mm pupil). Figure 6 presents the associated MTF's for the double-pass images in Fig. 5. As previously reported,[24,33] the estimated image quality is higher for the cases of parallel polarizers and significantly worse when crossed polarizers are placed in both paths. This is clearly shown in the MTF results: Those corresponding to the

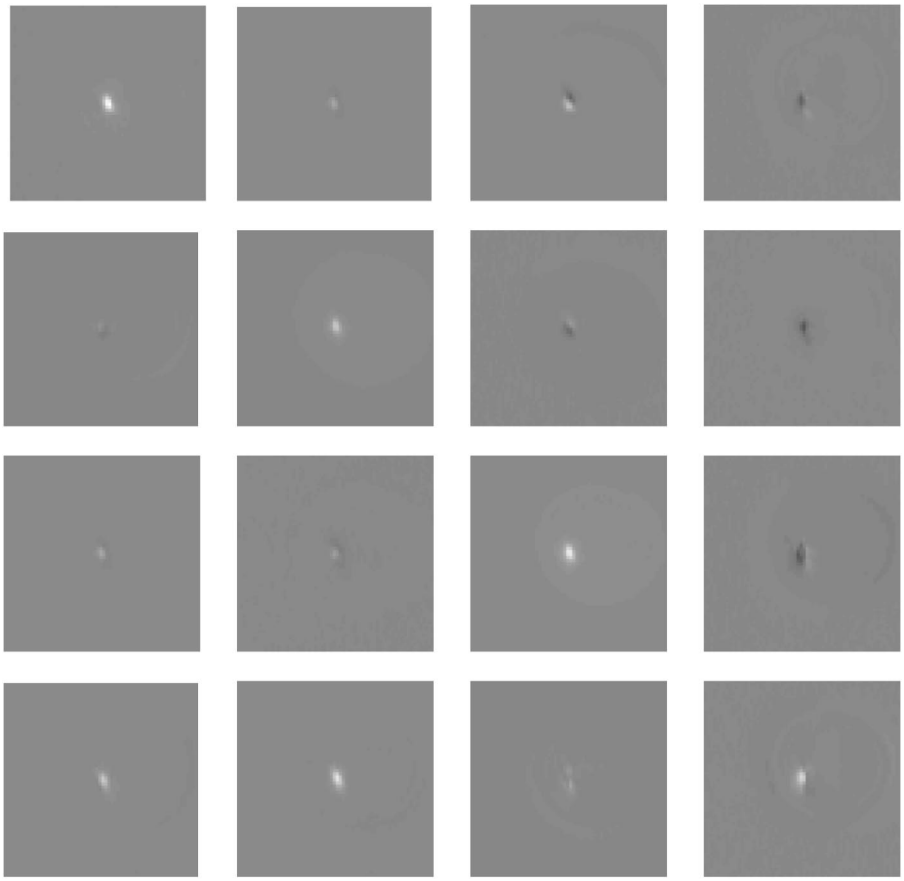

Fig. 3. Spatially resolved MM's for observer JB. Double-pass images with 2-mm pupil diameter were used. Each image subtends 59 arc min and corresponds to an element of the MM. Gray level ranges from −1 (black) to 1 (white). The MM in Ref. 27 corresponded to subject PA.

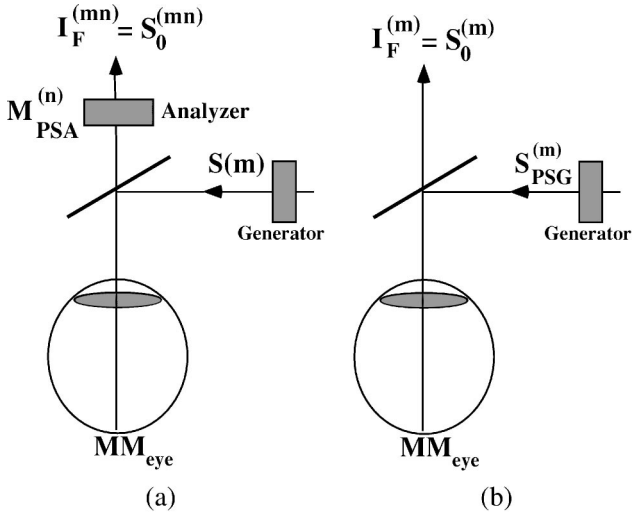

Fig. 4. Schematic diagrams of the reconstruction of double-pass images for (a) combinations of polarization states in both passes and (b) incident polarization states.

approximately crossed polarizers (HV and VH) are lower than for the parallel polarizers cases (HH and VV). Combinations of polarization states different from crossed linear states, as circular–horizontal (CH), may produce lower MTF's as well. These results show that if arbitrary polarizing elements are placed in both pathways of the apparatus, lower estimates of the MTF will be obtained, indicating that the retinal image quality obtained with the double-pass method depends strongly on the combination of polarization states in the first and second passes.

In Fig. 7(a) the averaged Strehl ratios for 2-mm reconstructed double-pass images in subject JB and six different PSG–PSA polarization states are shown. Figure 7(b) presents the mean for three subjects for the same combinations of polarization states.

B. Double-Pass Images Reconstructed for Light with Different Incident (Incoming Pass) Polarization States

Double-pass images reconstructed from the spatially resolved MM for different states of polarization in the light incident on the eye will indicate the effect of the polarization properties of the eye on the retinal image quality. In other words, those results will give information about the possibility that different retinal image quality could be produced with incident light of different polarization.

Since the elements M_{01}, M_{02} and M_{03} of the MM are not constant (see Fig. 3), double-pass images for incident light with different polarization—i.e., linear horizontal and vertical, ±45-deg linear and right and left circular—will not be exactly the same. The ocular optical performance is then dependent on polarization. Figure 8 shows examples of reconstructed double-pass images for two different subjects [rows (a) and (b)] and four different incident polarization states. Images in Fig. 8 present

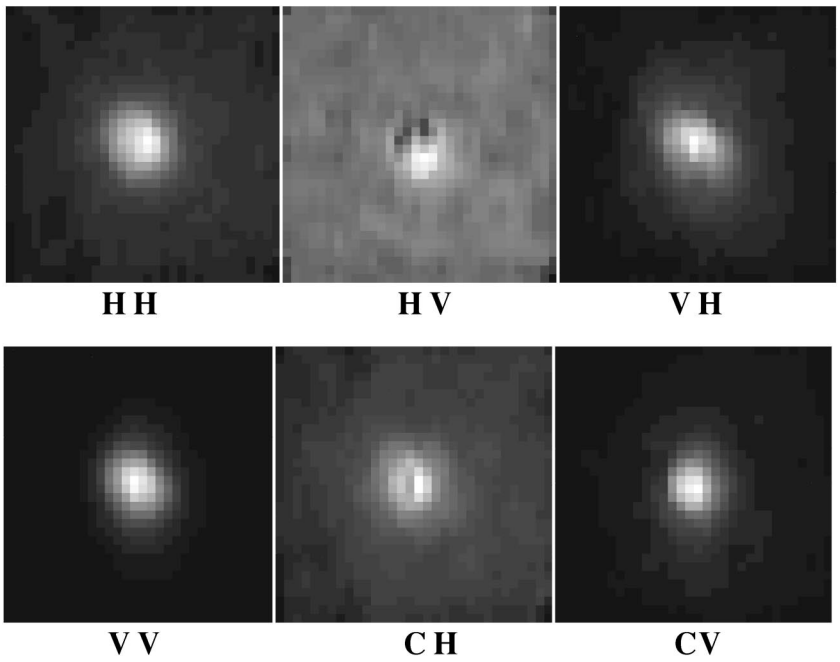

Fig. 5. Double-pass images reconstructed for different combinations of polarization states PSG–PSA: H, horizontal; V, vertical; C, right circular. Each image subtends 29 arc min of visual field.

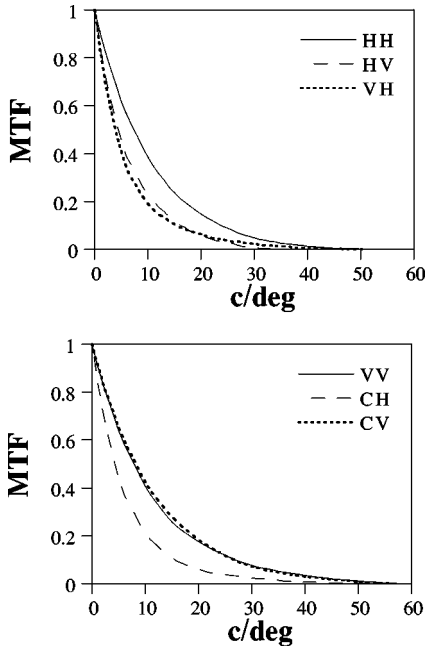

Fig. 6. MTF's corresponding to the double-pass images of Fig. 5.

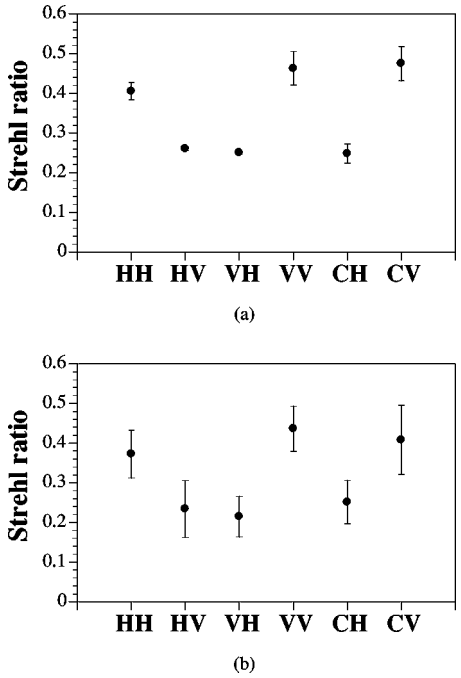

Fig. 7. Averaged Strehl ratios for reconstructed images (a) for subject JB with six different PSG–PSA polarization states and (b) for three different subjects. Error bars represent standard deviation.

small differences in the range of experimental errors during recording of double-pass images. This suggests that, although the retinal image depends on polarization, this dependence is weak. However, Fig. 8 presents double-pass images only for four particular polarization states. Consequently, one could ask what is the effect on ocular performance of any possible polarization state. This topic is addressed in Subsection 4.C.

C. Retinal Image Quality for Light with Any Incident (Incoming-Pass) Polarization State

Double-pass images were reconstructed for light incident on the eye with Stokes vectors covering the complete Poincaré sphere (with increments of 1 deg for azimuth χ and ellipticity ϕ). This represents virtually any possible polarization state incident on the eye. The MTF's and the Strehl ratio were computed from each of those double-pass images. For each subject and pupil diameter considered, the Stokes vectors that produced both the best and the worst retinal image were also obtained. With this procedure we estimated the range of variability of the retinal image quality that was due to polarization. Fig-

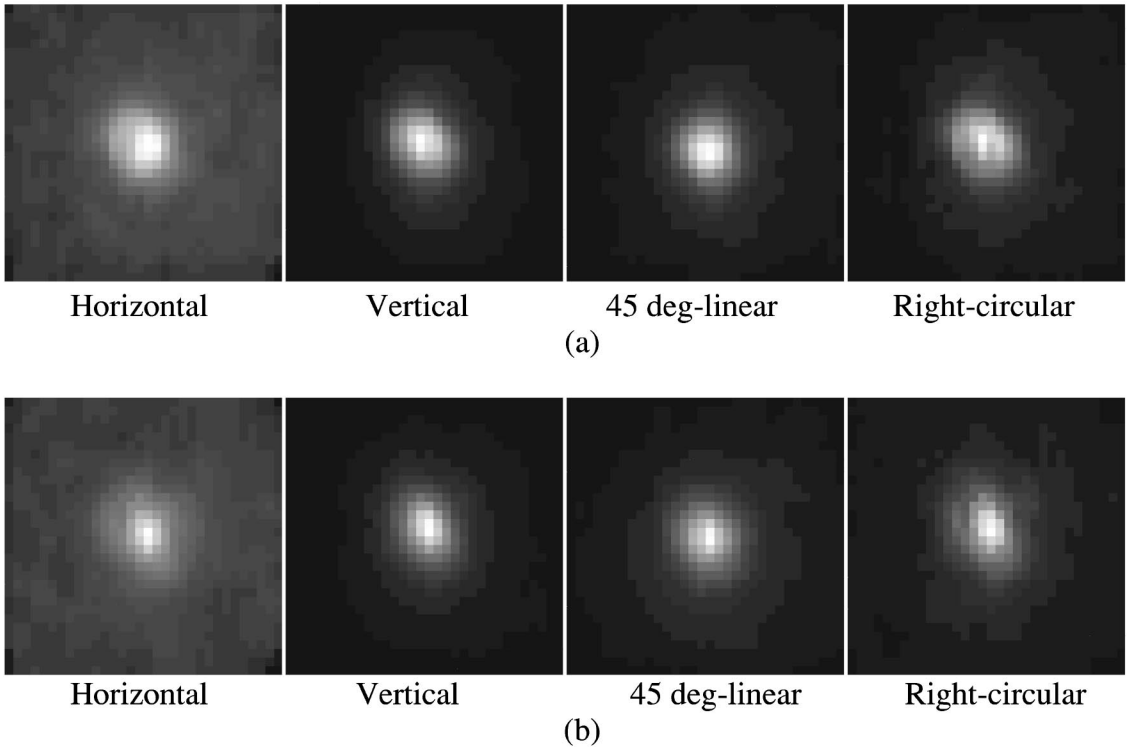

Fig. 8. Double-pass retinal images reconstructed (for 2-mm pupil diameter) with four different incoming polarization states for two different subjects. Each image subtends 29 arc min.

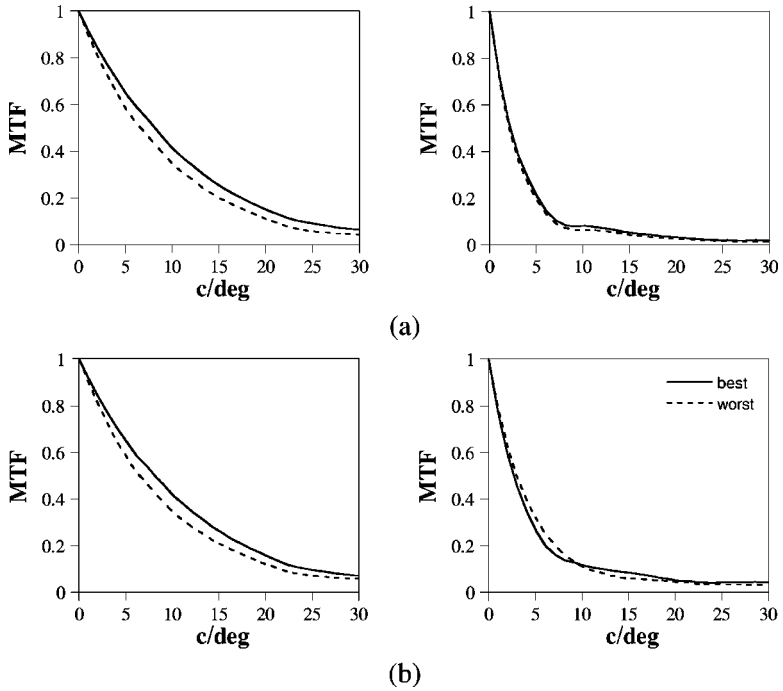

Fig. 9. Best and worst MTF's (a) for subject JB and (b) averaged for three subjects, with use of only incoming polarization states, for 2-mm (left) and 5-mm (right) pupil diameter.

ure 9(a) shows the best and the worst MTF's obtained by changing the polarization of the incoming light for subject JB (for two pupil diameters: 2 and 5 mm). The MTF's in Fig. 9(b) are the average for three subjects. All the other possible MTF's fall between those presented in the figure. The range of variability is quite small, especially for the larger pupil, as Fig. 10 shows. This suggests that light of different polarization states produces similar retinal images.

In addition, Stokes vectors producing both best and

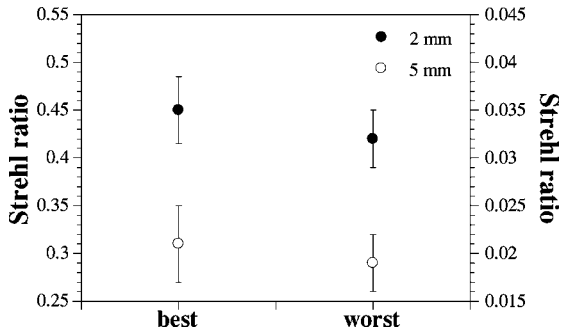

Fig. 10. Averaged Strehl ratios for best and worst MTF's for three subjects and two different pupil sizes: 2 mm, left scale; 5 mm, right scale. Error bars represent standard deviation.

worst MTF for a subject and a pupil diameter given were determined. Those Stokes vectors are shown in Fig. 11.

5. CONCLUSION AND SUMMARY

Since an incomplete extinction is obtained in the double-pass images with crossed polarizers, the eye necessarily changes the polarization state of the incident light. In addition, changes occurring in the central part and in the skirts of the images are different, thus having a possible effect on the estimates of retinal image quality. However, experiments that record images only with linear polarizers are not completely appropriate for understanding this problem. Moreover, they may lead to wrong interpretations (i.e., elliptical polarization would be incorrectly identified as partially depolarized light). In this sense, the idea[33] that the core of double-pass images remains polarized, while in the skirts of the image the light is nearly depolarized, although quite reasonable could not be fully demonstrated with that kind of experiment.

In the experiment present in this paper, images corresponding to parallel configuration are brighter than those associated with crossed configuration. This indicates that most of the light forming the image has not lost the original orientation; that is, it keeps the direction of the major axis of the ellipse of polarization entering the system.

The double-pass images recorded with different combinations of polarization states in the two passes are quite diverse. This indicates that different estimates of image quality can be obtained if uncontrolled polarizing elements are present in the setup. However, we showed that the effect of the polarization state of the incident light on the estimates of retinal image quality is small, probably within typical experimental variability. In addition, since the contribution of the corneal birefringence depends on each individual, the polarization state (Stokes vector) that produces images with best and worst image quality differs from one subject to another.

In summary, despite the complicated polarization properties of the human eye, the retinal image quality or, alternatively, the ocular aberrations is nearly independent of the state of polarization of the incident light. This means that it is not possible to improve the ocular optics by using a specific type of polarized light. As a consequence, the type of polarization used in the double-pass technique does not significantly affect the results. However, it should be noted that when polarizing elements are placed in both the first and the second passes, incorrect estimates of the image quality might be obtained.

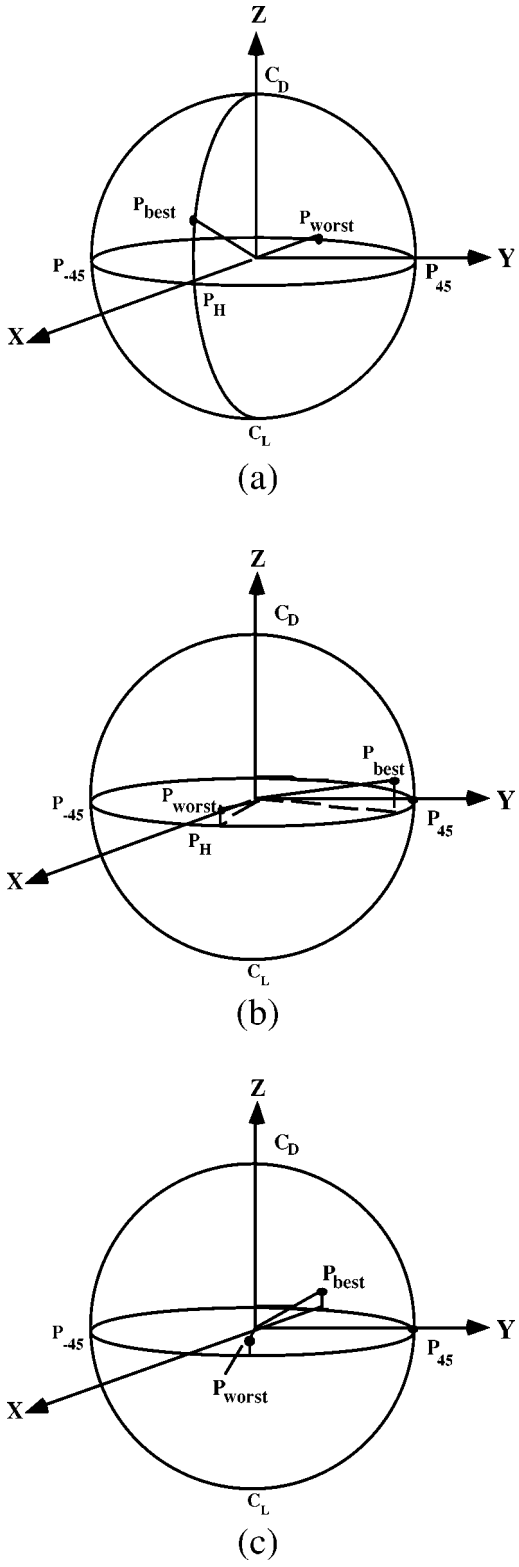

Fig. 11. Stokes vectors on the Poincaré sphere that produce images (2-mm pupil diameter) corresponding to both best and worst MTF's for each subject: (a) AG, (b) JB, (c) PA. P_H, $P_{\pm 45}$, C_R, and C_L are associated with linear horizontal, 45-deg linear and right- and left-circular polarization states, respectively.

ACKNOWLEDGMENTS

This research was supported by Dirección General de Enseñanza Superior (Spain) grant PB97-1056 to P. Artal.

The authors can be reached at the address on the title page or by e-mail: pablo@um.es (P. Artal) and bueno@um.es (J. M. Bueno).

REFERENCES

1. M. F. Flamant, "Étude de la répartition de lumière dans l'image rétinienne d'une fente," Rev. Opt. **34**, 433–459 (1955).
2. F. W. Campbell, and R. W. Gubisch, "Optical quality of the human eye," J. Physiol. (London) **186**, 558–578 (1966).
3. J. Santamaría, P. Artal, and J. Bescós, "Determination of the point-spread function of the human eye using a hybrid optical-digital method," J. Opt. Soc. Am. A **4**, 1109–1114 (1987).
4. P. Artal and R. Navarro, "Monochromatic modulation transfer function of the human eye for different pupil diameters: an analytical expression," J. Opt. Soc. Am. A **11**, 246–249 (1994).
5. J. A. M. Jennings and W. N. Charman, "Off-axis image quality in the human eye," Vision Res. **21**, 445–455 (1981).
6. D. R. Williams, P. Artal, R. Navarro, M. J. McMahon, and D. H. Brainard, "Off-axis optical quality and retinal sampling in the human eye," Vision Res. **36**, 1103–1114 (1996).
7. P. Artal, M. Ferro, I. Miranda, and R. Navarro, "Effects of aging in retinal image quality," J. Opt. Soc. Am. A **10**, 1656–1662 (1993).
8. P. Artal, S. Marcos, R. Navarro, I. Miranda, and M. Ferro, "Through focus image quality of eyes implanted with monofocal and multifocal intraocular lenses," Opt. Eng. **34**, 772–779 (1995).
9. N. López-Gil, I. Iglesias, and P. Artal, "Retinal image quality in the human eye as a function of the accommodation," Vision Res. **38**, 2897–2907 (1998).
10. W. N. Charman, "Optics of the human eye," in *Visual Optics and Instrumentation*, Vol. 1 of *Vision and Visual Dysfunction*, J. R. Cronly-Dillion, ed. (Macmillan, London, 1991), pp. 1–26.
11. G. J. van Blokland, "Ellipsometry of the human retina *in vivo*: preservation of polarization," J. Opt. Soc. Am. A **2**, 72–75 (1985).
12. A. Stanworth and E. J. Naylor, "The polarization optics of the isolated cornea," Br. J. Ophthamol. **34**, 201–211 (1950).
13. L. J. Bour and N. J. Lopes Cardozo, "On the birefringence of the living human eye," Vision Res. **21**, 1413–1421 (1981).
14. G. J. van Blokland and S. C. Verhelst, "Corneal polarization in the living human eye explained with a biaxial model," J. Opt. Soc. Am. A **4**, 82–90 (1987).
15. F. A. Bettelheim, "On the optical anisotropy of lens fiber cells," Exp. Eye Res. **21**, 231–234 (1975).
16. H. B. klein Brink, "Birefringence of the human crystalline lens *in vivo*," J. Opt. Soc. Am. A **8**, 1788–1793 (1991).
17. G. S. Brindley and E. N. Willmer, "The reflexion of light from the macular and peripheral fundus oculi in man," J. Physiol. **116**, 350–356 (1952).
18. H. L. de Vries, A. Spoor, and R. Jielof, "Properties of the eye with respect to polarized light," Physica **19**, 419–432 (1953).
19. R. A. Weale, "Polarized light and the human fundus oculi," J. Physiol. **186**, 925–930 (1966).
20. R. A. Bone, "The role of the macular pigment in the detection of polarized light," Vision Res. **20**, 213–219 (1980).
21. B. F. Hochheimer and H. A. Kues, "Retinal polarization effects," Appl. Opt. **21**, 3811–3818 (1982).
22. G. J. van Blokland and D. van Norren, "Intensity and polarization of light scattered at small angles from the human fovea," Vision Res. **26**, 485–494 (1986).
23. A. W. Dreher, K. Reiter, and R. N. Weinreb, "Spatially resolved birefringence of the retinal nerve fiber layer assessed with a retinal laser ellipsometer," Appl. Opt. **31**, 3730–3735 (1992).
24. D. R. Williams, D. H. Brainard, M. J. McMahon, and R. Navarro, "Double-pass and interferometric measures of the optical quality of the eye," J. Opt. Soc. Am. A **11**, 3123–3134 (1994).
25. J. Liang, B. Grimm, S. Goelz, and J. F. Bille, "Objective measurement of wave aberrations of the human eye with the use of a Hartmann–Shack wave-front sensor," J. Opt. Soc. Am. A **11**, 1949–1957 (1994).
26. J. Liang and D. R. Williams, "Aberrations and retinal image quality of the normal human eye," J. Opt. Soc. Am. A **14**, 2873–2883 (1997).
27. J. M. Bueno and P. Artal, "Double-pass imaging polarimetry in the human eye," Opt. Lett. **24**, 64–66 (1999).
28. American National Standard for the Safe Use of Lasers ANSI Z136.1 (Laser Institute of America, Orlando, Fla., 1993).
29. J. M. Bueno, "Measurement of parameters of polarization in the living human eye using imaging polarimetry," Vision Res. **40**, 3791–3799 (2000).
30. J. L. Pezzaniti and R. A. Chipman, "Mueller matrix imaging polarimetry," Opt. Eng. **34**, 1558–1568 (1995).
31. J. P. McGuire, Jr., and R. A. Chipman, "Diffraction image formation in optical systems with polarization aberrations. I: Formulation and example," J. Opt. Soc. Am. A **7**, 1614–1626 (1990).
32. P. Artal, I. Iglesias, N. López-Gil, and D. G. Green, "Double-pass measurements of the retinal image quality with unequal entrance and exit pupil sizes and the reversibility of the eye's optical system," J. Opt. Soc. Am. A **12**, 2358–2366 (1995).
33. W. N. Charman, "Reflection of plane-polarized light by the retina," Br. J. Physiol. Opt. **34**, 34–49 (1980).